

Evaluation of data transfer influence in coupled Monte Carlo finite element model on microstructure evolution predictions

WERMIŃSKI Mariusz^{1,a *}, PERZYŃSKI Konrad^{1,b}, SITKO Mateusz^{1,c}
and MADEJ Łukasz^{1,d}

¹AGH University of Science and Technology, 30 Mickiewicza Avenue, 30-059 Krakow, Poland

^amarwer@agh.edu.pl, ^bkperzyns@agh.edu.pl, ^cmsitko@agh.edu.pl, ^dlmadej@agh.edu.pl

Keywords: Interpolation, Monte Carlo, Finite Element Method, Welding

Abstract. The processes of microstructure evolution under thermal loading occurring during welding or additive manufacturing are highly complex and challenging to observe experimentally. Therefore, in this work, to support experimental investigation, a hybrid numerical model based on the combination of the Monte Carlo (MC) and Finite Element (FE) method was developed to simulate both temperature profiles and corresponding grain growth phenomena at a micro scale explicitly. The welding simulation was selected as a case study. The discrete MC microstructure evolution model is based on the temperature distribution provided by the FE simulation with the Goldak heat source model. The temperature data are transferred from 3D FE space to cubic MC Pott's domain in each time step. Direct coupling between the MC cells and FE cubic elements provides accurate results but significantly increases the simulation time. Therefore, coarser FE meshes are used in the research, but this requires applying reliable data interpolation techniques between the two methods. As a result, the temperature field stored in a coarse FE cloud of points is interpolated into regular high-resolution MC cell space in each time step. Evaluation of the influence of various interpolation methods, along with their parameters on the final microstructure morphology after welding, is presented within this work.

Introduction

Modern industry requires efficient and durable methods of joining various metallic parts. The most popular techniques in this area are the welding operations [1], which are based on melting both materials in the joining zone by the focused heat sources, e.g. laser or electron based. However, similar material processing routes are also used in other applications like additive manufacturing or soldering [2,3]. Despite the final application, phenomena controlling microstructure evolution in all those processes are very complex to analyze experimentally. During the high-heat loading of metallic materials, various phenomena should be considered, involving melting, crystallization, grain growth, phase transformation, etc. Most of the time, experimental observations of these phenomena are done after the end of the process. As a result, drawing direct conclusions about local microstructure behavior during the process is not straightforward. Therefore, numerical simulations are frequently used to support experimental observations and visualize phenomena that are difficult or impossible to observe in laboratory conditions [4].

To investigate both the temperature evolution and corresponding microstructural changes in the welding and heat-affected zones, a hybrid Finite Element (FE) - Monte Carlo (MC) model was developed. The FE part based on the classical Goldak movable heat source model is responsible for the evaluation of the temperature fields during the process. The MC model is used as a full-field approach allowing explicit representation of complex grain morphology in the weld line area [5–7]. The MC method was selected in this case due to a straightforward definition of cell transition rules. However, in this case, coupling both methods is a crucial stage in successful model development.



The direct coupling assumes linking each cubic FE element with a corresponding cubic MC cell, as presented in Fig. 1a. In this case, the data transfer is straightforward as both computational domains operate on the space discretized exactly in the same way. However, a high-resolution MC space is required to capture the grain growth during the process, which directly leads to a high-resolution FE mesh. As a result, the computational times for large-scale models may be quite excessive. Therefore, the solution is to use a coarser FE mesh that does not directly correspond to the MC cells. However, in this case, the data transfer between the two incompatible meshes in each time step has to be developed based on the interpolation technique, as seen in Fig. 1b.

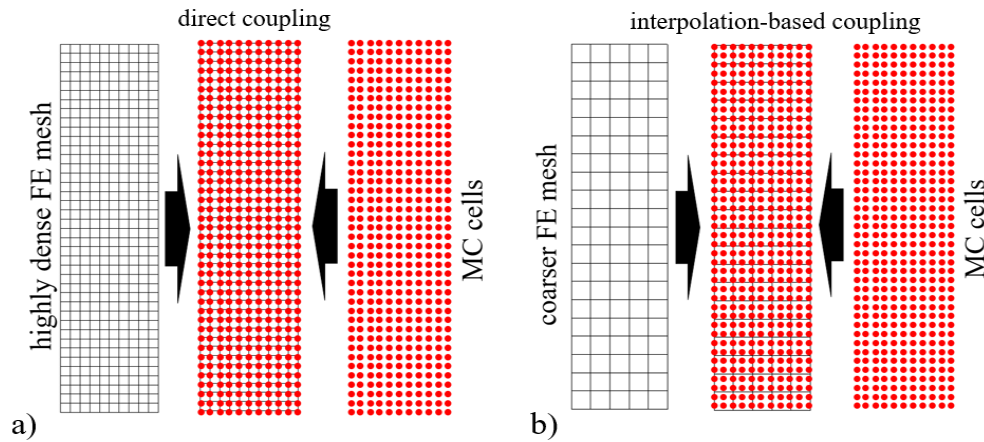


Fig. 1. Concepts of the FE-MC models based on a) direct and b) interpolation-based coupling.

Evaluation of the influence of various interpolation methods and their parameters on the final microstructure morphology after welding simulated by the MC model is the primary goal of the current research to confirm the quality of the results.

Hybrid FE-MC Model Description

The essential step in simulating the effect of thermal loading on the microstructure evolution during welding is to acquire sensible temperature data in specified conditions. The presented approach assumes that the thermal loading during welding is performed by the moving heat source incorporated into the FE framework. The welding operation of two high-purity aluminium plates was selected as a case study for the current investigation. The applied moving heat source model is based on Goldak's ellipsoid [8] in the form of:

$$q(x, y, z, t) = \frac{6\sqrt{3}Q}{abc\pi\sqrt{\pi}} e^{\frac{-3x^2}{a^2}} e^{\frac{-3y^2}{b^2}} e^{\frac{-3[z+v(\tau-t)]^2}{c^2}} \quad (1)$$

where: q – heat flux at a given point in the coordinate system; a , b , c – semi-axes of the ellipsoid; Q – energy input rate; v – welding velocity; τ – lag factor.

The FE model provides information on the temperature evolution during the subsequent process stages, as presented in Fig. 2.

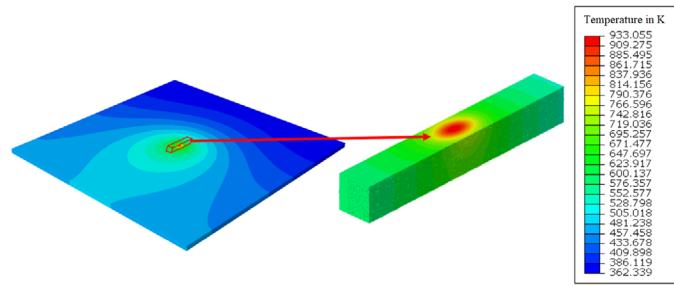


Fig. 2. FE temperature field in [K] during welding with the highlighted section of interest for interpolation analyses.

The acquired data for a particular time step is called a frame in the current work. Data from each frame has to be then transferred to the regular cubic MC space. To reduce the computational time, the MC space is associated only with the heat-affected zone during the welding.

The developed MC microstructure evolution model is based on Pott's approach [9]. The initial microstructure morphology required for simulation (Fig. 3) is generated using the cellular automata grain growth algorithm from the DigiCore library [10]. The average grain diameter is 0.143 [mm], and the resolution of generated MC space is $102 \times 92 \times 701$, with the cell's edge length set to 0.02 [mm] to properly capture grain boundaries geometry (Fig. 3). The main idea of the MC method is to calculate the probability p of, a randomly selected, cell state change and set it to a new state according to the following equation:

$$p = \begin{cases} M(T_i) e^{\frac{-\Delta E}{kT}} & \Delta E \leq 0 \\ M(T_i) & \Delta E > 0 \end{cases} \quad (2)$$

where: ΔE – change in the energy; kT – model factor; $M(T_i)$ – grain mobility; T_i – temperature of a cell.

The Eq. 3 describes change in the free energy:

$$\Delta E = E_{new} - E \quad E = \sum_{j=1}^Z 1 - \delta_{ss_j} \quad (3)$$

where: E – free energy for an initial state, E_{new} – free energy for a new state, Z – number of neighbors, δ – Kronecker delta of state between current and neighboring cell. The probability p is calculated for every cubic cell in MC space. This computation is applied for every FE frame of welding simulation by performing an arbitrary set number of iterations known as the Monte Carlo Steps (MCS).

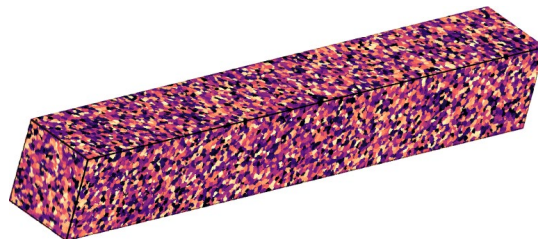


Fig. 3. Initial microstructure.

The temperature field from the FE model is used to calculate the grain mobility $M(T_i)$, which involves activation energy Q for specific material and given temperature T_i of MC cell in Arrhenius equation (Eq. 4). In the current model Eq. 4 is normalized to 0 – 1 range by M_0 scaling factor, where 1 means the value for a melting point:

$$M(T_i) = M_0 e^{-\frac{Q}{kT_i}} \quad (4)$$

Data transfer between the two models is performed by interpolating temperature values from FE cloud of points into regular high-resolution 3D MC space. As pointed out, selecting appropriate interpolating functions is crucial to reproduce a final microstructure representation after welding. Four different methods were implemented and used in the current FE-MC hybrid model. The first is an Inverse Distance Weighting (IDW) method [11]. This approach is based on the evaluation of the temperature value in a particular cell by averaging the values of neighboring FE data points (Eq. 5). The weights from Eq. 6 depend on the distance and the parameter n (Eq. 6):

$$u(x) = \begin{cases} \frac{\sum_{i=1}^N w_i(x) u_i}{\sum_{i=1}^N w_i(x)} & d(x, x_i) \neq 0 \\ u_i & d(x, x_i) = 0 \end{cases} \quad (5)$$

$$w_i(x) = \frac{1}{d(x, x_i)^n} \quad (6)$$

The second interpolation algorithm is based on Smoothed-Particle Hydrodynamics (SPH) approach [12], where the evaluated value u depends on the weighting kernel function k (Eq. 7). The kernel function determines the weight of value using the neighborhood radius r and distance d between the current point x and neighboring one x_i . Two different kernel functions: *Epanechnikov* (Eq. 8) and *Quartic* (Eq. 9), were used during the current investigation:

$$u(x, r) = \frac{\sum_{i=1}^N k(x_i, r) u_i}{\sum_{i=1}^N k(x_i, r)} \quad (7)$$

$$k_{\text{epanechnikov}}(x, r) = \frac{3}{4} \left(1 - \left(\frac{x}{r} \right)^2 \right) \quad (8)$$

$$k_{\text{quartic}}(x, r) = \frac{15}{16} \left(1 - \left(\frac{x}{r} \right)^2 \right)^2 \quad (9)$$

Additionally, two other approaches are considered due to their simplicity and low computational complexity. The third interpolation method is a particular variant of the IDW method with n set to 0. This provides a simple average method (AVG) that only takes unweighted values into the computations. The last interpolation technique is based on finding the nearest point and applying its value (NEAREST).

Comparison of Interpolation Methods

In order to study the impact of interpolation methods and their parameters on the evolution of microstructure in the MC space, two simulations of the thermal loading of an aluminium plate were carried out. The first computation was made with the most time-consuming direct coupling where FE points are equidistant from each other, and the size of the FE elements is the same as MC cells (Fig. 1a). In this case, the data are directly transferred from the particular FE integration point into the corresponding MC cell, and there is no interpolation. The simulation results from Fig. 4 are assumed to be a benchmark for further investigation. The second set of simulations is realized on a coarser FE mesh, and as described earlier, different interpolation methods were used to transfer the data into the MC model.



Fig. 4. Final microstructure obtained from the direct coupling between FE and MC models.

Each interpolation test was then conducted according to the parameters collected in Table 1. Corresponding final microstructure morphologies from hybrid FE-MC simulations are gathered in Fig. 5 – 9. For presentation purposes, only the middle section of the heat-affected zone is presented. Besides that, skeletonization of the top view of the microstructure was done to emphasize the difference in the shape of grains. Finally, obtained computational times and average grain sizes are summarized in Table 2.

Table 1. Combination of applied interpolation methods and their parameters.

Case no.	1	2	3	4	5	6	7	8	9	10	11	12	13
Interpolation method	IDW	IDW	IDW	SPH/Q	SPH/Q	SPH/Q	SPH/E	SPH/E	SPH/E	AVG	AVG	AVG	NEAREST
Radius of range	0.2	0.4	0.4	0.2	0.4	0.8	0.2	0.4	0.8	0.2	0.4	0.8	-
<i>n</i> parameter	2	1	2	-	-	-	-	-	-	-	-	-	-

Table 2. The results of applied interpolation methods and reference microstructure.

Case no.	1	2	3	4	5	6	7	8	9	10	11	12	13	Ref.
Average computation time per frame [s]	46	46	45	21	22	20	4	4	3	18	21	26	17	-
Average central grain area [mm ²]	0.012	0.03	0.018	0.013	0.029	0.032	0.014	0.033	0.033	0.035	0.037	0.029	0.031	0.043
Average elongated grain area [mm ²]	0.030	0.108	0.085	0.062	0.127	0.168	0.083	0.148	0.162	0.123	0.147	0.123	0.134	0.167

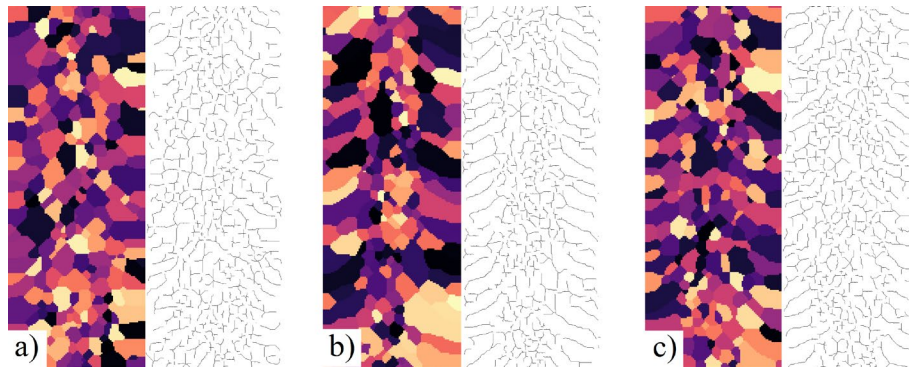


Fig. 5. Top view of the microstructure and its skeletons after thermal loading using IDW method: a) Case 1, b) Case 2, c) Case 3.

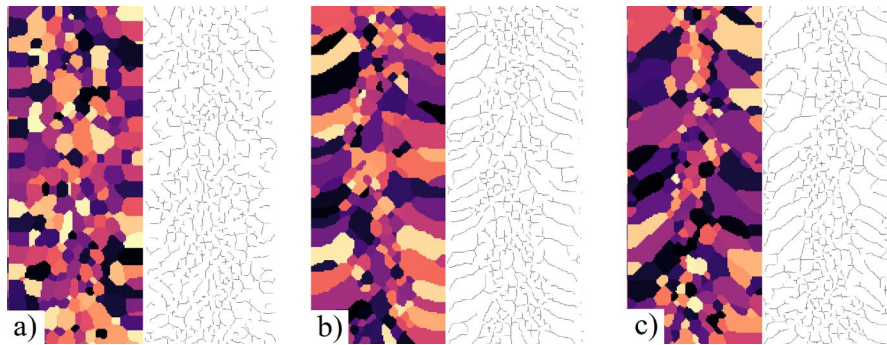


Fig. 6. Top view of the microstructure and its skeletons after thermal loading using SPH-Quartic method: a) Case 4, b) Case 5, c) Case 6.

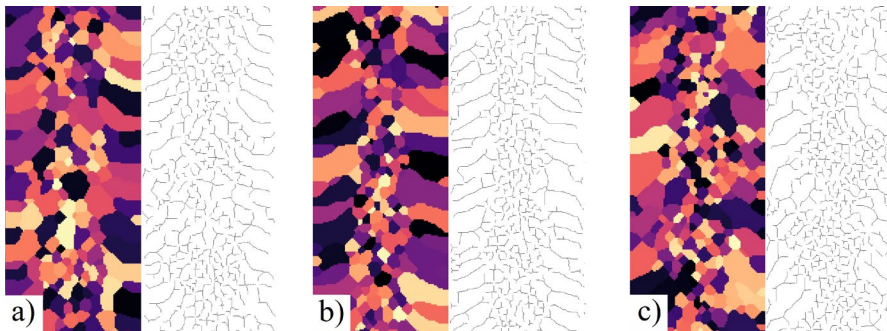


Fig. 7. Top view of the microstructure and its skeletons after thermal loading using SPH-Epanenchnikov method: a) Case 7, b) Case 8, c) Case 9.

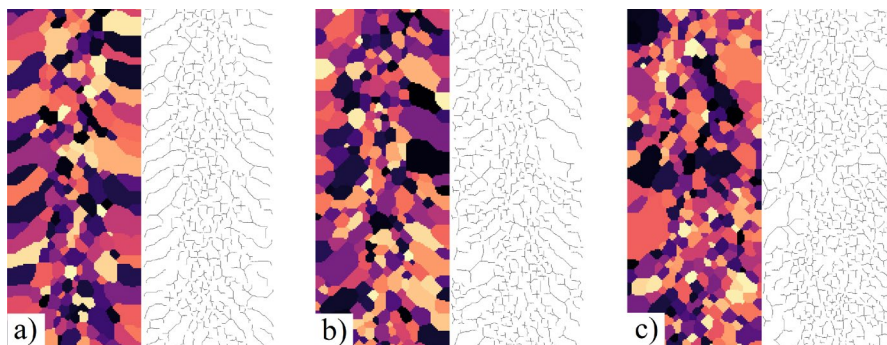


Fig. 8. Top view of the microstructure and its skeletons after thermal loading using AVG method: a) Case 10, b) Case 11, c) Case 12.

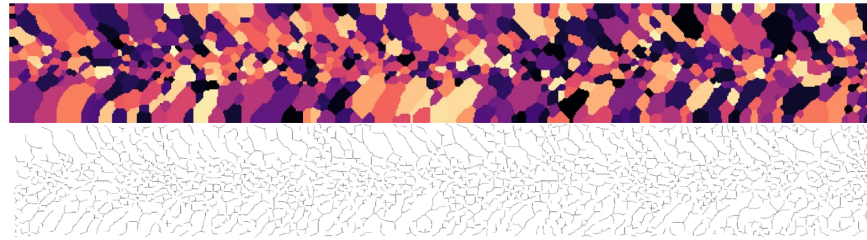


Fig. 9. Top view of the microstructure and its skeletons microstructure after thermal loading using NEAREST method (Case 13, entire model).

As presented, the applied methods and their parameters highly impact the resulting microstructures. Presented top views of the microstructures (Fig. 5 – 9) can be easily distinguished into two sections: the central part, which results in new and not fully grown grains, and the second one, with elongated grains after the grain growth. This division is particularly evident in the presented skeletons. Size, curvature, and a fraction of elongated grains depend on selected interpolation algorithms and their parameters. It is observed that SPH method in both variants produces the most elongated and curved shapes of grains that are related to the number of points taken into account in the neighborhood. However, at 0.8 [mm] neighborhood radius, the shapes of elongated grains are more irregular. According to the AVG method, if fewer values are considered in the averaging, the final structure is similar to the referenced one. The IDW approach shows the curvature of grains depends on the number of points taken into consideration, and the size relies on a parameter n value. The NEAREST method, despite its simplicity, provides a very similar microstructure to the reference one. From the presented approaches, similar microstructures are produced by the SPH (Fig. 6b and Fig. 7b), the AVG (Fig. 8a), and the NEAREST. These methods differ in two points: the shape and size of elongated grains, which are the largest in the SPH, and the angle of direction of grain growth from the fusion zone to HAZ boundary, which is more perpendicular in the case of SPH and AVG. These methods present significantly different results from the reference, especially regarding the elongated-to-center grains ratio. Despite this, it seems that the NEAREST method most closely reflects the reference microstructure relative to the others.

Summary

Based on the presented research, it can be concluded that:

- 1) temperature fields mapped from macro to micro scale by interpolation methods slightly vary from the direct transfer case. There are also minor differences in the shape and size of new grains.
- 2) the most similar microstructure can be obtained by using an appropriately tailored method. The most effective results are produced using SPH interpolation (using *Epanechnikov* and *Quartic* kernel functions with 0.4 radii of range), AVG method (with the application of 0.2 radii of range) and the nearest neighbor approach. NEAREST provides the closest results to the benchmark case among these three methods.
- 3) approaches based on averaging (all cases of the IDW and the AVG second and third case) introduce some disorder in temperature fields, which results in a lack of elongated grains.

More simulations will be carried out on a larger computational MC domain as the subject of future work. The research will also include an examination of geometric parameters and velocity of the heat source and its influence on the microstructure evolution.

Acknowledgement

The financial assistance of the National Science Centre project No. 2019/35/B/ST8/00046 is acknowledged.

References

- [1] B. Wang, S.J. Hu, L. Sun, T. Freiheit, Intelligent welding system technologies: State-of-the-Art review and perspectives, *J. Manuf. Syst.* 56 (2020) 373-391. <https://doi.org/10.1016/J.JMSY.2020.06.020>
- [2] A.V. Müller, D. Dorow-Gerspach, M. Balden, M. Binder, B. Buschmann, B. Curzadd, T. Loewenhoff, R. Neu, G. Schlick, J.H. You, Progress in additive manufacturing of pure tungsten for plasma-facing component applications, *J. Nucl. Mater.* 566 (2022) 153760. <https://doi.org/10.1016/J.JNUCMAT.2022.153760>
- [3] S. Mercan, The effect of the amount of soldering wire on fatigue strength in joining steels and sockets, *Int. J. Fatigue* 127 (2019) 157–164. <https://doi.org/10.1016/J.IJFATIGUE.2019.06.004>
- [4] J. Yanagimoto, D. Banabic, M. Banu, L. Madej, Simulation of metal forming – visualization of invisible phenomena in the digital era, *CIRP Annals* 71 (2022) 599-622. <https://doi.org/10.1016/J.CIRP.2022.05.007>
- [5] F. Villaret, B. Hary, Y. de Carlan, T. Baudin, R. Logé, L. Maire, M. Bernacki, Probabilistic and deterministic full field approaches to simulate recrystallization in ODS steels, *Comput. Mater. Sci.* 179 (2020) 109646. <https://doi.org/10.1016/J.COMMATSCI.2020.109646>
- [6] C.L. Park, P.W. Voorhees, K. Thornton, Application of the level-set method to the analysis of an evolving microstructure, *Comput. Mater. Sci.* 85 (2014) 46-58. <https://doi.org/10.1016/J.COMMATSCI.2013.12.022>
- [7] D. Tournet, H. Liu, J.L. Lorca, Phase-field modeling of microstructure evolution: Recent applications, perspectives and challenges, *Prog. Mater. Sci.* 123 (2022) 100810. <https://doi.org/10.1016/J.PMATSCI.2021.100810>
- [8] J. Goldak, A. Chakravarti, M. Bibby, A new finite element model for welding heat sources, *Metall. Mater. Trans. B* 15 (1984) 299-305. <https://doi.org/10.1007/BF02667333>
- [9] A. Williamson, J.P. Delplanque, Investigation of Dynamic Abnormal Grain Growth Using the Monte Carlo Potts method, *Comput. Mater. Sci.* 124 (2016) 114-129. <https://doi.org/10.1016/J.COMMATSCI.2016.07.025>
- [10] K. Boguń, M. Sitko, M. Mojżeszko, L. Madej, Cellular automata-based computational library for development of digital material representation models of heterogenous microstructures, *Archiv. Civ. Mech. Eng.* 21 (2021) 61. <https://doi.org/10.1007/s43452-021-00211-9>
- [11] P.M. Bartier, C.P. Keller, Multivariate interpolation to incorporate thematic surface data using inverse distance weighting (IDW), *Comput. Geosci.* 22 (1996) 795-799. [https://doi.org/10.1016/0098-3004\(96\)00021-0](https://doi.org/10.1016/0098-3004(96)00021-0)
- [12] L.D.G. Sigalotti, O. Rendón, J. Klapp, C.A. Vargas, F. Cruz, A new insight into the consistency of the SPH interpolation formula, *Appl. Math. Comput.* 356 (2019) 50-73. <https://doi.org/10.1016/j.amc.2019.03.018>